

# Influence of novel ammonium-modified zinc-free phosphate nanofillers on anticorrosive features of primer-less polyurethane top-coating compositions

Krzysztof Kowalczyk, Katarzyna Przywecka, Barbara Grzmil

© The Author(s) 2018

**Abstract** Anticorrosive polyurethane coating compositions were compounded using novel zinc-free nanosized phosphates: aluminum ammonium phosphates (AAP) or calcium aluminum ammonium phosphates (CAAP). For comparison, a nanosized strontium phosphate (SP), AAP/SP mixtures, and a microsized zinc phosphate (ZP) were tested. Paints containing ammonium-modified phosphates exhibited similar or a slightly higher viscosity than systems with SP or ZP. Nevertheless, coatings with the AAP or CAAP reached significantly better gloss and adhesion to a steel substrate as well as a slightly higher hardness. Results of a salt spray test showed that anticorrosive properties of the coatings containing AAP/SP mixtures were markedly better in relation to the systems containing solely AAP, CAAP, SP, or ZP. Electrochemical tests revealed the best barrier/anticorrosive features for AAP (electrochemical impedance spectroscopy and potentiodynamic polarization) or SP and CAAP (a novel electrochemical noise technique).

**Keywords** Calcium aluminum ammonium phosphate, Strontium phosphate, Zinc phosphate, Anticorrosive paint, Electrochemical noise

## Introduction

Since application of red lead and zinc chromate (VI) in anticorrosive coating materials has been prohibited, zinc phosphates belong to the most effective protective fillers/pigments used in 1 K and 2 K paints for steel substrates. However, due to lately revealed negative influence of these fillers on aquatic life, various zinc phosphates, pyrophosphates, and phosphosilicates modified with Li,<sup>1</sup> Na,<sup>2</sup> Mg,<sup>3</sup> Al,<sup>3–14</sup> K,<sup>15</sup> Ca,<sup>3,6,16</sup> Fe,<sup>4,12,14</sup> Sr,<sup>6,17–19</sup> and/or Mo<sup>4,6,14,20</sup> were developed and investigated in solventborne, low-VOC, and water-thinnable coating compositions. Additionally, many types of zinc-free derivatives of phosphorus-based acids and ammonium and/or Al,<sup>5,7–9,15,16</sup> Mg,<sup>18</sup> Ca,<sup>3,10,13,16</sup> Cr, Mn,<sup>16</sup> Sr,<sup>5,10,13,17,19,21</sup> Ba,<sup>15,17</sup> Pb<sup>12</sup> were investigated as corrosion inhibitors in coating systems. Anticorrosive efficiency of the mentioned fillers (in relation to the zinc phosphates) is a result of a type of polymeric binder, auxiliary fillers addition as well as investigation method, e.g., electrochemical measurements of fillers aqueous extracts or filled coatings, accelerated tests in salt spray, condensation or Kesternich chambers, immersion tests, outdoor exposition. Generally, it could be claimed that various phosphates containing Zn and Al,<sup>4,5,13,14</sup> Sr,<sup>19</sup> Fe,<sup>4,12,14</sup> or Ca<sup>6</sup> belong to the most attractive corrosion inhibiting additives. A positive influence of Ca cations on aluminum zinc phosphate efficacy was described in the literature.<sup>3</sup> In the case of Zn-free compounds, aluminum phosphates<sup>16,22</sup> and these additionally modified with Sr<sup>13,21</sup> exhibit relatively high protective features. Interestingly, polyurethane coatings filled with nanosized aluminum phosphates (Ø255–270 nm) or submicrosized aluminum ammonium phosphates (500–990 nm) reached similar or better anticorrosive properties than samples with a microsized zinc aluminum phosphate (< 63 µm)<sup>7–9</sup> and an aluminum phosphate (< 4 µm). It is noteworthy that the men-

---

K. Kowalczyk (✉)  
Polymer Institute, Faculty of Chemical Technology and Engineering, West Pomeranian University of Technology in Szczecin, Pułaskiego 10, 70-322 Szczecin, Poland  
e-mail: kkowalczyk@zut.edu.pl

K. Przywecka, B. Grzmil  
Institute of Chemical and Environment Engineering, Faculty of Chemical Technology and Engineering, West Pomeranian University of Technology in Szczecin, Pułaskiego 10, 70-322 Szczecin, Poland

tioned nanofillers improved gloss of the coatings<sup>7</sup>; that optical feature is crucial for compositions applied as primer-less top-coating systems. In the case of anticorrosive epoxy systems (containing bisphenol-based resins<sup>1,2,4,5,14,16,21</sup>), the cured coatings must be additionally covered by a UV-resistant paint due to their chalking during exterior exposure.

In this work, novel nanosized ammonium-modified Zn-free phosphate fillers (i.e., two aluminum ammonium phosphates and two calcium aluminum ammonium phosphates) were tested as anticorrosive components in primer-less solventborne 2 K polyurethane coating compositions. Prepared systems were compared to the paints based on a nanosized strontium phosphate and a commercial microsized zinc phosphate; additionally, mixtures of the aluminum ammonium phosphates and strontium phosphate were examined. The  $\Lambda$  parameter value (i.e., pigment volume concentration/critical pigment volume concentration = 0.55) for the prepared coatings was applied according to the literature data.<sup>23</sup>

## Materials and methods

### Preparation of the anticorrosive polyurethane paints

The following components were used for solventborne 2 K polyurethane paints preparation:

- WorléeCryl A2218, solution of hydroxyacrylic resin, viscosity ca. 1 250 mPa·s, hydroxyl value 58 mg KOH/g (on solids) (Worlée-Chemie, Germany);
- Tolonate HDB-LV, hexamethylene diisocyanate derivative, viscosity ca. 2 000 mPa·s, NCO content 23.5 wt% (Perstorp, Sweden);
- aluminum ammonium phosphates (AAP-1 and AAP-2; ZUT, Poland);
- calcium aluminum ammonium phosphates (CAAP-1 and CAAP-2; ZUT);
- strontium phosphate (SP; ZUT);
- zinc phosphate (ZP) (FC-M2, Złoty Stok Farby, Poland) as a reference Zn-based anticorrosive filler;
- titanium dioxide (TiO<sub>2</sub>), specific gravity ( $\rho$ ) 4.1 g/cm<sup>3</sup>, oil absorption (OA) 21 g/100 g (Tytanpol R001, G.A.Z.Ch. Police, Poland);
- mica/quartz mixture,  $\rho = 2.75$  g/cm<sup>3</sup>, OA = 35 g/100 g (Aspolit F40, Aspanger Bergbau, Austria);
- wollastonite treated with an alkylsilane,  $\rho = 2.85$  g/cm<sup>3</sup>, OA = 40 g/100 g (Tremin 939-300 FST, Quarzwerke, Germany);
- talc,  $\rho = 2.75$  g/cm<sup>3</sup>, OA = 49 g/100 g (Finntalc M03-SQ, Mondo Minerals, Finland);
- xylene (90 wt%) and butyl acetate (10 wt%) mixture as a solvent (POCh, Poland);
- wetting/dispersing additive based on unsaturated

polycarboxylic acid polymer (BYK-P 104S, BYK-Chemie, Germany);

- silicone defoamer (BYK-067A, BYK-Chemie).

The paints were prepared as follows: A phosphate filler, TiO<sub>2</sub>, and Aspolit F40 were dispersed (25°C, 25 min) in a part of hydroxyacrylic resin containing the auxiliary additives and solvent in the pearl mill (Klaxon, UK). Then, the talc and wollastonite were incorporated and the system was milled for 20 min. The paste was mixed with the rest of the hydroxyacrylic component using the laboratory dissolver (1250 rpm, 1 h) (VMA Getzmann, Germany), filtered (190  $\mu$ m), and mixed with the aliphatic diisocyanate hardener using a laboratory mixer and stored at RT for 20 min before application. The paint components, phosphate fillers content, pigment volume concentration (PVC), and critical pigment volume concentration (CPVC) values are specified in Table 1. The paints were applied with a brush (according to the Polish Standard PN-C-81514:1979) and leveled with a spiral film applicator (150  $\mu$ m) onto a steel substrate. The steel panels (Q-Panels, Q-Lab Europe, England) with the dimensions of 76 × 152 mm (for adhesion and electrochemical impedance spectroscopy (EIS) tests) and 102 × 152 mm (salt spray test) were used. Two-layer samples were prepared by applying two layers of coating compositions with 24-h painting interval. The paints were also applied onto glass plates (for hardness measurements) using a gap applicator (300  $\mu$ m). The coatings were cured at room temperature for 14 days before testing.

### Test methods

#### Characterization of the phosphate fillers

The specific gravity of the phosphate fillers was measured using Ultrapyc 1200e helium autopycnometer (Quantachrome Inst., USA). The oil absorption for the mentioned phosphates was measured according to the Polish standard PN-EN ISO 787-5. The particle size of the fillers was analyzed using the laser scanning microscope VK-9700 (Keyence, USA). The conductivity of phosphate aqueous dispersions (5 wt%) was tested using the Elmetron CC-505 conductometer (Elmetron, Poland). The pH of aqueous suspensions (10 wt%) of the phosphate fillers was measured by means of Elmetron CP-401 pH meter. Chemical composition of the nanofillers was determined by colorimetric vanadium–molybdenum method (P<sub>2</sub>O<sub>5</sub> content; Spekol 11, Carl Zeiss, Germany), spectrometric ICP-AES method (aluminum, strontium, zinc, and calcium content; Optima 5300 DV, PerkinElmer, USA) as well as using the ion selective electrode Orion 11–35 (ammonium content).

Electrochemical noise experiments for the uncoated steel substrate (Q-Panel) were performed using EN120

**Table 1: Composition of the polyurethane paints**

Paint acronym Phosphate acronym	P-AA1 AAP-1	P-AA2 AAP-2	P-CAA1 CAAP-1	P-CAA2 CAAP-2	P-S SP	P-AAS1 AAP-1 + SP <sup>a</sup>	P-AAS2 AAP-2 + SP <sup>a</sup>	P-Z ZP
Pigment volume content (vol%)								
Mica/quartz					35			
TiO <sub>2</sub>					15			
Wollastonite					10			
Talc					10			
Phosphate					30			
Phosphate content <sup>b</sup> (wt%)	8.6	9.2	10.5	10.2	15.3	11.3	11.7	17.5
Phosphate content <sup>b</sup> (vol%)	5.8	6.4	7.2	6.9	7.7	6.7	6.8	7.1
PVC	19.3	21.1	24.0	22.9	25.7	22.2	22.9	26.3
CPVC	35.1	38.4	43.6	41.6	46.7	40.4	41.7	47.8
A <sup>c</sup>	0.55							

<sup>a</sup>Mixture of an aluminum ammonium phosphate and strontium phosphate (50/50 m/m); <sup>b</sup>phosphate filler content in a cured coating; <sup>c</sup>PVC/CPVC

software and FAS2 femtostat working in ZRA mode (i.e., as a zero resistance ammeter) (Gamry, USA). Two steel samples were installed on both sides of a horizontal glass cell filled with 0.1 wt% suspension of a phosphate filler in 3.5 wt% NaCl aqueous solution (prepared 24 h before the test). The cell was equipped with a saturated calomel reference electrode, continuously aerated using compressed oil-free air and placed in a Faraday cage. The whole test consisted of thirteen measurements (with 2 h intervals) of current flow fluctuations between the identical steel samples (sample area of 3.14 cm<sup>2</sup>); each measurement was carried out for 1024 s (sampling intervals of 1 s). The current noise density as a value of the root mean square (RMS) of amplitude of current flow density (registered for all the measurements) as well as a total charge value (in relation to the density of current flow noise) was automatically calculated by the Echem Analyst software (Gamry). The corrosion inhibition efficiency ( $\eta_{EN}$ ) of the phosphate fillers was calculated according to the following equation:

$$\eta_{EN} = \left[ \frac{q_0 - q}{q_0} \right] \times 100(\%),$$

where  $q_0$  and  $q$  are charge density values for the steel substrates tested in 3.5 wt% NaCl aqueous solution and 0.1 wt% suspension of a phosphate filler in the 3.5 wt% NaCl aqueous solution, respectively.

Steel corrosion products formed during electrochemical noise tests as well as powdered phosphate fillers were investigated using Fourier-transform infrared spectroscopy with attenuated total reflectance (ATR) accessories (Nexus FTIR; Thermo Nicolet, USA).

The X-ray analysis of the steel corrosion products was carried out using Empyrean PANalytical diffractometer (Cu K $\alpha$ , 10–70° 2 $\theta$ ) equipped with the HighS-

core + Philips software and ICDD PDF-4 + 2015 database.

Tafel experiments ( $\pm 250$  mV in relation to OCP, scan rate 0.25 mV/s) for the uncoated steel substrate were performed using DC105 software and FAS2 femtostat. As a result, corrosion potential and corrosion current density values were determined by means of Echem Analyst software. Steel polarization was carried out using electrolytes prepared by shaking a phosphate filler (0.1 g) with 100 g of 3.5 wt% NaCl aqueous solution for 24 h; then, the suspension was filtered. The Tafel tests were performed after 2 min of a vertical glass cell filling with the phosphate extract. The corrosion inhibition efficiency ( $\eta_{TAF}$ ) of phosphate extracts was calculated according to the equation:

$$\eta_{TAF} = \left[ \frac{i_0 - i}{i_0} \right] \times 100(\%),$$

where  $i_0$  and  $i$  are corrosion current density values registered for the steel substrate tested in 3.5 wt% NaCl aqueous solution and an aqueous extract of phosphate filler in the 3.5 wt% NaCl aqueous solution, respectively.

#### Characterization of the paints and cured coatings

High shear viscosity tests (I.C.I. cone-plate system; Research Equipment, UK) were performed for ready-to-use liquid coating compositions (i.e., after 20 min since incorporation of the hardener). Gloss at 85° (PN-EN ISO 2813, three measurements for each sample; IQ20/60/85 glossmeter, Rhopoint Inst., UK), König pendulum hardness (PN-EN ISO 1522, three measurements for each sample; AWS-5, Dozafil, Poland) were evaluated on cured paints. Pull-off adhesion of coatings (PN-EN ISO 4624:2004, six measurements for each composition; 510-T hydraulic apparatus, Elcometer,

UK) was measured before and after 250 h of the samples immersion in a periodically air-saturated NaCl aqueous solution (3.5 wt%). The thickness of cured films was measured with the electronic film gauge Byko-test 8500 (BYK-Gardner, Germany) according to PN-EN ISO 2808. EIS tests were carried out with coated panels (two-layer coatings with a thickness of 128–147  $\mu\text{m}$ , three samples of each composition) after 0, 100, and 250 h of their immersion in the periodically air-saturated NaCl aqueous solution (3.5 wt%). A three-electrode vertical glass cell (with 14.5  $\text{cm}^2$  surface sample area) equipped with a graphite counter electrode and a saturated calomel reference electrode was used inside the Faraday cage. The impedance data (0.001–10,000 Hz, 100 mV amplitude of sinusoidal voltage vs. OCP) were collected using EIS300 software with FAS2 femtostat (Gamry) and analyzed using the electric circuit model presented in Fig. 1 ( $R_u$ —uncompensated solution resistance,  $R_p$ —pore resistance,  $C_c$ —coating capacitance<sup>24</sup>). The pore resistance and coating capacitance parameters were calculated in respect to the coating thickness and presented as relative  $R_p$  (i.e.,  $R_{pr}$ ,  $\Omega/\mu\text{m}$ ) and relative  $C_c$  ( $C_{cr}$ ,  $\text{F}/\mu\text{m}$ ) with standard deviations.

The salt spray test was carried out according to PN-EN ISO 9227 in CorrosionBox 400 (Co.fo.me.gra., Italy) using a NaCl aqueous solution (concentration of  $50 \pm 5$  g/l) sprayed with compressed oil-free air. The back side and edges of the steel panels with x-cut coatings (according to EN ISO 17872) were protected, and the samples were mounted at the angle of 20° vertically. The temperature in the spray cabinet was maintained at 35°C.

## Results and discussion

The viscosity values of the prepared polyurethane paints are presented in Fig. 2. The compositions filled with aluminum ammonium phosphates (AAP-1 or AAP-2) were significantly more viscous (900 and 820 mPa·s, respectively) in relation to the systems with calcium aluminum ammonium phosphates (650 and 670 mPa·s), strontium phosphate (530 mPa·s), and zinc phosphate (670 mPa·s). It should be noted that the analyzed parameter was not affected by the fillers particles size (Table 2). For example, diameters of AAP-1 (283 nm, 900 mPa·s) and CAAP-1 (298 nm,

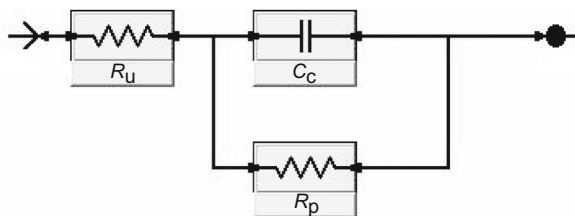


**Fig. 1:** Electric circuit model for coatings immersed in 3.5 wt% NaCl aqueous solution

650 mPa·s) were quite similar. Nevertheless, viscosity of the paints depended on the oil adsorption number (OA) of the tested phosphate fillers and their content in the coating compositions. The highest OA and the lowest phosphate volumetric content were noted for AAP-1 (160 g/100 g, 5.8 vol.%). Considering the other compositions with nanosized phosphates, these with the strontium phosphate (the lowest OA and the highest volumetric content) reached the lowest viscosity. On the other hand, cured coatings containing the aluminum ammonium phosphates exhibited significantly higher gloss (92 G.U. for P-AA1 and 86 G.U. for P-AA2; Fig. 2) in relation to the systems with the CAAP-type fillers (77 and 81 G.U.) or SP (62 G.U.). However, application of AAP/SP mixtures (weight ratio 50:50, volumetric ratio ca. 60:40) markedly reduced viscosity of the liquid compositions (in comparison with these containing only AAP-1 or AAP-2), and gloss of the prepared coatings was not so significantly diminished (85 G.U. for P-AAS1 and 82 G.U. for P-AAS2). It should be noticed that the former parameter values recorded for the AAP/SP-based paints (i.e., 680 and 650 mPa·s) and the paint filled with microsized zinc phosphate (P-Z, 670 mPa·s,  $\varnothing 2.8$   $\mu\text{m}$ ; Table 2) were similar. On the other hand, gloss of the coating with ZP was much lower (65 G.U., Fig. 2) in comparison with P-AAS1 and P-AAS2. Reduced gloss of cured coatings containing a microsized anticorrosive filler (in comparison with samples with nanosized phosphates) was previously observed and described in the literature.<sup>7</sup> Due to relatively high gloss values of the samples filled with ammonium-modified phosphates ( $\geq 77$  G.U.), these systems can be applied as highly decorative protective coatings.

Generally, coatings filled with the zinc-free phosphates exhibited markedly higher hardness than the sample with ZP (Fig. 3). These with the aluminum ammonium phosphates (P-AA1, P-AA2) reached 13–14 hardness units after 1 day of curing at RT (10 a.u. was noted for P-Z). After 14 days since application of the AAP-based layers, their hardness was higher (61 a.u.) in relation to the system with zinc phosphate (54 a.u.) and samples with the other phosphates (57–60 a.u.) as well. Due to a relatively high hardness of the coating with strontium phosphate (60 a.u. after 14 days), the samples containing mixtures of that filler with the aluminum ammonium phosphates reached quite high values of that parameter (58 a.u. for P-AAS1 and 60 a.u. for P-AAS2). Interestingly, the highest hardness was noted for the samples containing aluminum ammonium phosphates; however, volumetric content of AAP-1 (5.8 vol.%) and AAP-2 (6.4 vol.%) in the coatings was lower in comparison with the CAAP-type (7.2 and 6.9 vol.%), SP (7.7 vol.%), or ZP filler (7.1 vol.%). The mentioned coating with AAP-1 filler (P-AA1) was characterized by the higher average pull-off adhesion values (3.6 MPa before and 3.4 MPa after immersion for 250 h in a brine) in comparison with the other samples; it is noteworthy that pure cohesive-type failures were observed for all

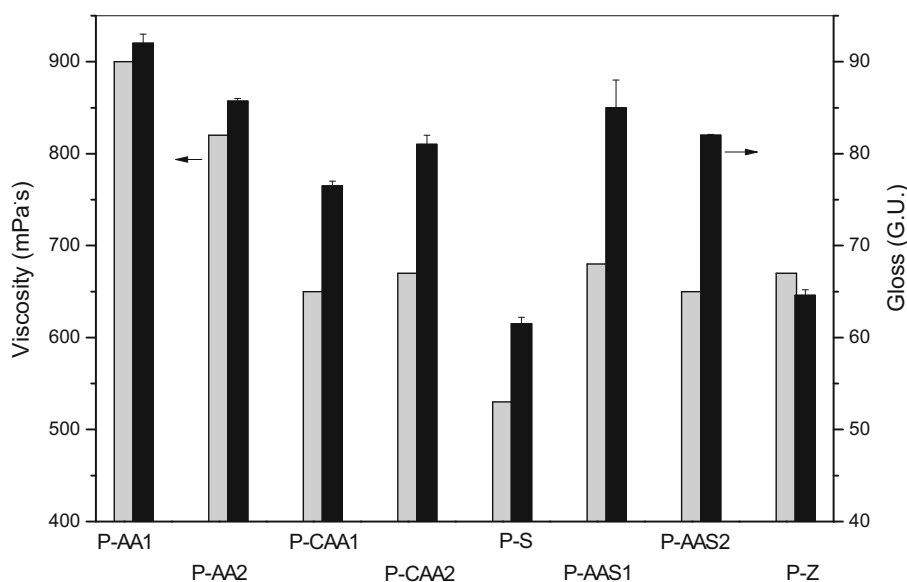


Fig. 2: Viscosity of liquid paints and gloss of cured polyurethane coatings

Table 2: Physical and chemical properties of the phosphate fillers

Phosphate acronym	AAP-1	AAP-2	CAAP-1	CAAP-2	SP	ZP
Density (g/cm <sup>3</sup> )	2.11	2.13	2.16	2.24	3.2	3.7
Oil adsorption (g/100 g)	160	123	74	89	36	27
Average particle diameter (nm)	283 ± 128	334 ± 87	298 ± 45	310 ± 42	356 ± 116	2800 ± 2600
Water solubility (wt%)	0.93	0.93	0.72	0.55	0.23	0.44
Electrical conductivity <sup>a</sup> (μS/cm)	2900	1720	3200	2130	193	47
pH <sup>a</sup>	6.7	7.8	5.6	7.1	7.6	7.2
P <sub>2</sub> O <sub>5</sub> content (wt%)	44.4	43.3	36.2	39.8	34.0	37
Al content (wt%)	12.4	13.2	6.7	7.2	0	0
Ca content (wt%)	0	0	12.1	13.7	0	0
NH <sub>3</sub> content (wt%)	4.6	6.0	2.3	3.2	0	0
Sr content (wt%)	0	0	0	0	44.8	0
Zn content (wt%)	0	0	0	0	0	42

<sup>a</sup>Conductivity and pH of aqueous extracts of a phosphate filler

tested coatings. Slightly lower adhesion/cohesion was recorded for P-CAA2 (3.4 and 3.0 MPa, respectively). In the case of samples with the aluminum ammonium phosphates (or with the calcium aluminum ammonium phosphates), higher cohesion of P-AA1 (or P-CAA2)—before its immersion in the brine—was probably a result of the lower volumetric content of AAP-1 (CAAP-2) than AAP-2 (CAAP-1; Table 1) in the coatings; dissipated nanoparticles of the phosphates might act as steric hindrances disturbing/limiting crosslinking process of the polymeric matrix (mainly in the samples with a higher nanofiller content, i.e., in P-AA2 and P-CAA1). After immersion in the NaCl aqueous solution (250 h), average cohesion values for P-AA2 and P-CAA1 (as well as for the other coatings) were slightly increased, e.g., from 2.7 to 3.1 MPa for the former sample. Perhaps it was caused by a reaction between the partially unreacted iso-

cyanate curing agent and water penetrating into the coatings (and creation of urea linkages). It should be mentioned that pull-off adhesion of the coating systems (exhibiting the highest initial values of that parameter: P-AA1 and P-CAA2) was reduced after their immersion in the brine. In these cases, the water molecules penetrating the samples were not consumed via their reaction with –NCO groups, but they plasticized the polymeric binder of the layers and/or weakened hydrogen bonds between polymer chains. It is noteworthy that the polyurethane coating modified with the microsized zinc phosphate exhibited significantly lower adhesion (2.1 and 2.5 MPa) in relation to the other systems (Fig. 4).

Generally, the adhesion values recorded for the coatings (after the immersion test) correlate with EIS test results. The sample with the highest adhesion (P-AA1) was characterized by the highest relative pore

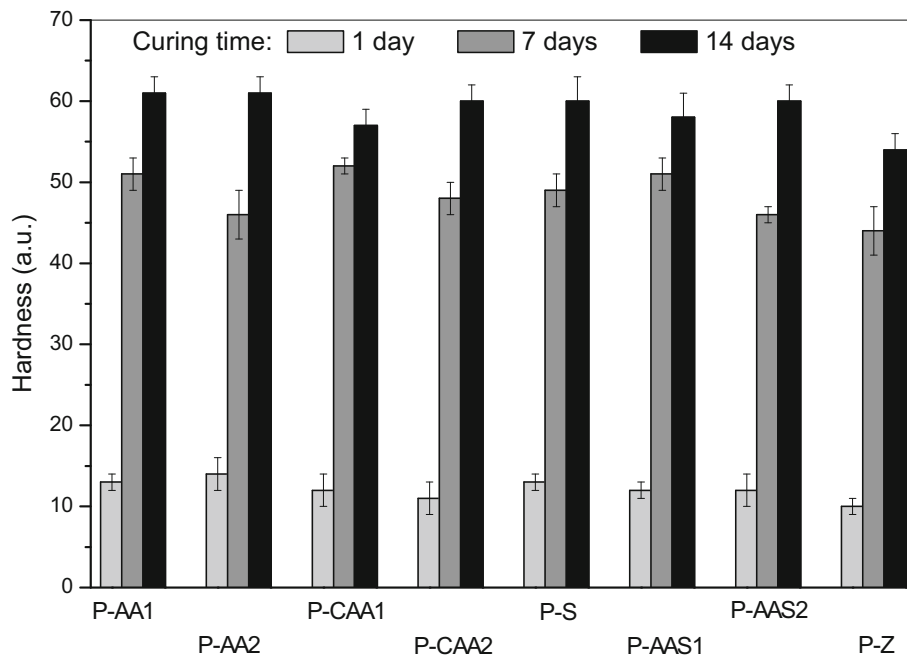


Fig. 3: Hardness of cured polyurethane coatings

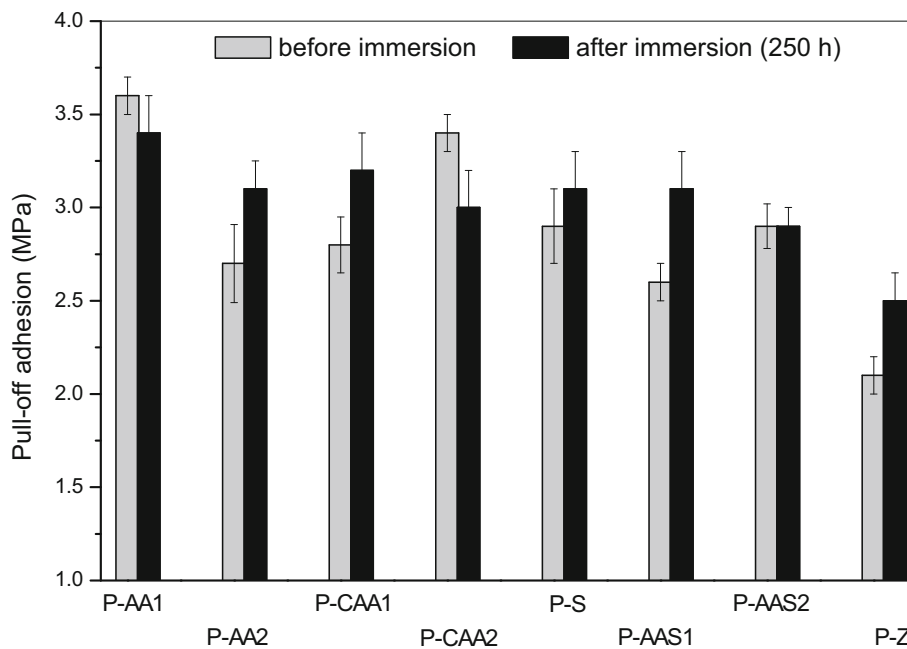


Fig. 4: Pull-off adhesion of cured polyurethane coatings (before and after immersion in 3.5 wt% NaCl aqueous solution)

resistance ( $R_{pr}$ : 604 and 29.6  $M\Omega/\mu m$ ; Fig. 5) and the lowest relative coating capacitance ( $C_{cr}$ : 4.6 and 11.6  $pF/\mu m$ ; Fig. 6) measured before and after immersion in the NaCl aqueous solution (250 h). In contrast, the most reduced barrier features were noted for the sample with micro-sized zinc phosphate; the lowest value of  $R_{pr}$  and the highest value of  $C_{cr}$  (after the immersion test) were revealed for P-Z sample

(0.12  $M\Omega/\mu m$  and 19.2  $pF/\mu m$ , respectively). Exemplary Bode plots for P-AA1 and P-Z coatings are presented in Fig. 7. Interestingly, in the case of coatings with the ammonium-modified phosphates, i.e., AAP and CAAP-type fillers,  $R_{pr}$  (250 h) depends on volumetric content of the anticorrosive additives; the highest  $R_{pr}$  was recorded for P-AA1 (29.6  $M\Omega/\mu m$ , 5.8 vol.% of AAP1), while the lowest for P-CAA1

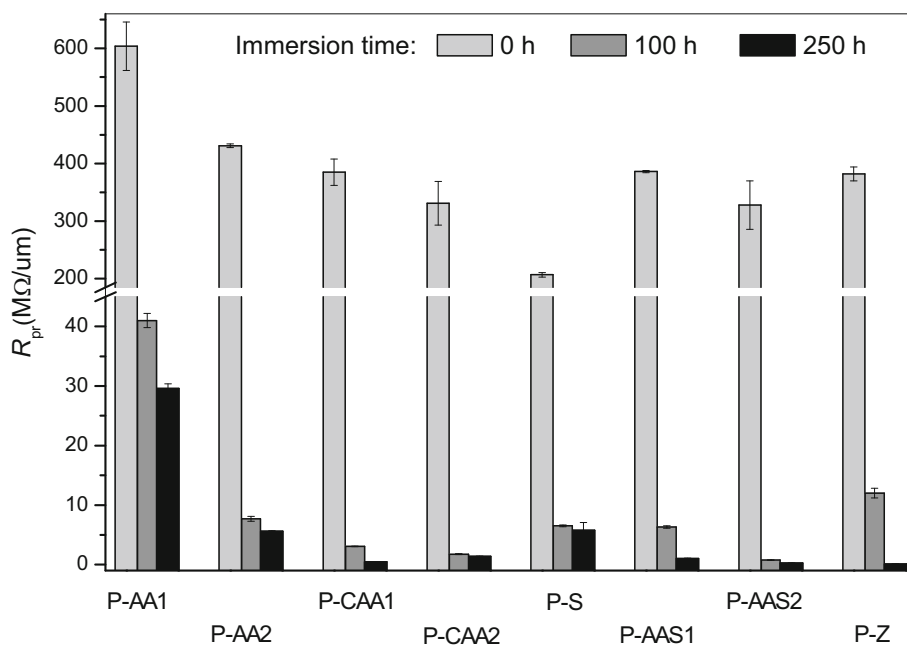


Fig. 5: Relative pore resistance ( $R_{pr}$ ) of coatings immersed in 3.5 wt% NaCl aqueous solution

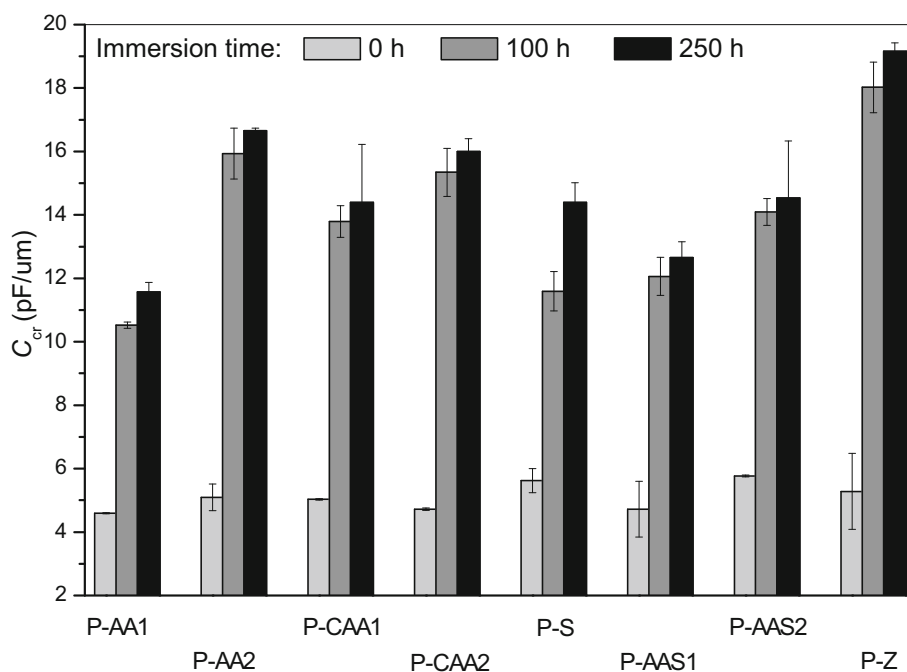


Fig. 6: Relative coating capacitance ( $C_{cr}$ ) of coatings immersed in 3.5 wt% NaCl aqueous solution

(0.45  $M\Omega/\mu m$ , 7.2 vol.% of CAAP-1). The similar relation can be observed for the samples containing AAP-1/SP and AAP-2/SP mixtures (P-AAS1 and P-AAS2). However, the AAP-type phosphates exhibit similar solubility in water (Table 2); the higher volumetric content of AAP-2 in P-AA2 and P-AAS2 (in comparison with AAP-1 concentration in P-AA1 and P-AAS1) resulted in more effective dissolution of

AAP-2 particles (in water absorbed during the immersion test) and higher  $R_{pr}$  reduction. On the other hand,  $C_{cr}$  (250 h) of the coatings with ammonium-modified phosphates was (probably) affected by particles diameters of the applied phosphates; P-AA1 reached the lowest  $C_{cr}$  (11.6  $pF/\mu m$ ,  $\varnothing 283$  nm), while the highest value was recorded for P-AA2 (16.7  $pF/\mu m$ , 334 nm). The coating filled with AAP-1/SP mixture was also

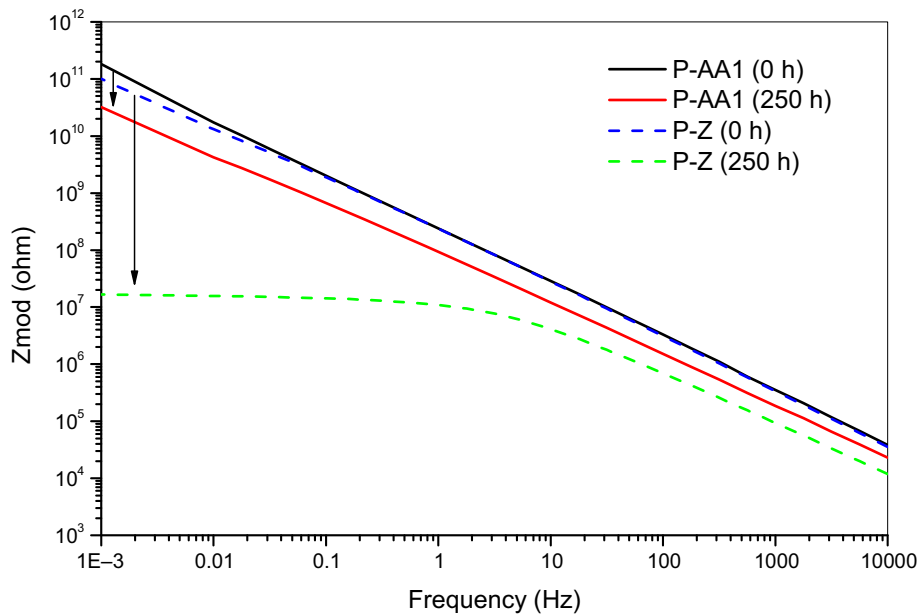


Fig. 7: Bode plots for P-AA1 and P-Z coatings before (0 h) and after immersion in 3.5 wt% NaCl aqueous solution (250 h)

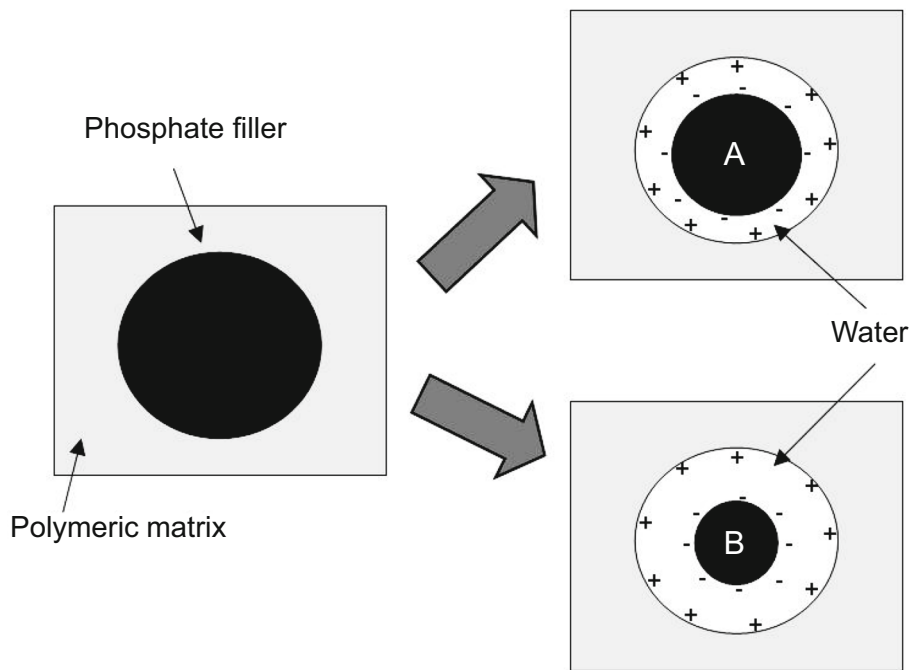


Fig. 8: Graphical model of spherical capacitors creation process from phosphate fillers with lower (A) and higher water solubility (B)

characterized by the lower  $C_{cr}$  (12.7 pF/ $\mu\text{m}$ ) in comparison with the sample with AAP-2/SP (14.5 pF/ $\mu\text{m}$ ). Nevertheless, the highest  $C_{cr}$  was observed for the sample with microsized zinc phosphate (19.2 pF/ $\mu\text{m}$ , 2800 nm). Perhaps a few particles of the tested phosphates acted as cores of spherical capacitors formed in the coatings during their immersion in the brine; it is known that capacitance of the capacitor (C)

(e.g., a coating pore with an occluded filler particle; Fig. 8) directly depends on a radius value of an interior sphere/core ( $R_1$ ) and increases with decreasing radius value of a shell sphere ( $R_2$ )<sup>25</sup>:

$$C = 4\pi\epsilon \left[ \frac{R_1 R_2}{R_2 - R_1} \right] (F).$$

In the case of fillers exhibiting similar water solubility, a coarse-grained phosphate filler (e.g., AAP-2, 334 nm; Table 2) should create a spherical capacitor with a higher capacitance value ( $C_{cr} = 16.7$  pF/ $\mu$  for P-AA2) than a fine-grained filler (AAP-1; 283 nm, 11.6 pF/ $\mu$ ). Considering phosphate fillers with similar particles diameters, higher capacitance should be observed for the sample with a low-solubility phosphate (e.g., P-CAA2; 310 nm, water solubility: 0.55 wt%,  $C_{cr} = 16.0$  pF/ $\mu$ ) than for the system with a more hydrophilic phosphate (P-CAA1, 298 nm, 0.72 wt%, 14.4 pF/ $\mu$ ). Arguably, electrical permittivity of a capacitor spacer ( $\epsilon$ ) (i.e., water or a filler aqueous solution) significantly influenced the registered capacitance values.

EIS data ( $R_{pr}$  and  $C_{cr}$ ) do not correlate with the salt spray test results (Table 3; Fig. 9). The lowest delamination around the scribe (after 480, 960, and 1440 h of coated samples exposition) was registered for the coatings filled with AAP-2/SP mixture (P-AAS2; 4.4–6.4 mm) and CAAP-2 (P-CAA2; 4.9–7.1 mm); the highest values of that parameter (1440 h) were noted for P-AA1 (10.5 mm) and P-CAA1 (11.0 mm). It should be noted that the samples (P-AA1 and P-CAA1) were also markedly blistered outside the scribe after exposure in the salt fog chamber (Table 3). Interestingly, P-AA1 exhibited the best barrier features according to EIS data, i.e., the highest  $R_{pr}$  (604–29.6 M $\Omega$ / $\mu$ m; Fig. 5) and the lowest  $C_{cr}$  values (4.6–11.6 pF/ $\mu$ m; Fig. 6) in relation to the other systems (431–0.12 M $\Omega$ / $\mu$ m and 4.7–19.2 pF/ $\mu$ m). It is noteworthy that the lowest  $R_{pr}$  and the highest  $C_{cr}$  values (250 h) were revealed for the sample with zinc phosphate; that coating reached moderate delamination around the scribe during exposure in the salt spray cabinet (5.8–8.4 mm; Table 3). That microsized filler was also characterized by the medium values of current noise density (292 nA/cm<sup>2</sup>) and corrosion inhibition efficiency (85%) calculated by means of electrochemical noise data (Table 4; Fig. 10); better anticorrosive features were noted for SP (146 nA/cm<sup>2</sup>, 92%), CAAP-1 (190 nA/cm<sup>2</sup>, 89%), and CAAP-2 filler (246 nA/cm<sup>2</sup>, 86%).

As mentioned above, the coatings filled with CAAP-2, i.e., P-CAA2, (or with the mixture of AAP-2 and SP; P-AAS2) exhibited the best anticorrosive features during their investigation in the salt spray chamber. It is noteworthy that delamination around the scribe was lower for the sample with CAAP-2 (or AAP-2) than for the coating based on CAAP-1 (AAP-1); probably it was a result of higher pH values of aqueous extracts of CAAP-2 and AAP-2 (caused by a higher NH<sub>3</sub> content in these fillers; Table 2). In the case of the coatings with mixed phosphates (P-AAS2; pH 7.8 for AAP-2 and pH 7.6 for SP), a synergistic effect occurred. Higher protective efficiency of epoxy coatings filled with strontium aluminum polyphosphates (in relation to zinc phosphate-based coatings) was revealed in the literature<sup>21</sup>; probably it was caused by precipitation of a protective layer (containing Fe, Sr, and P) on a steel substrate.

Interestingly, Tafel test outcomes (Table 4; Fig. 11) do not completely correlate with the EN data and the salt spray chamber test results. The highest corrosion inhibition efficiency ( $\eta_{TAF}$ ) was recorded for AAP-2 (68%), AAP-1/SP mixture (50%), and AAP-1 (47%). It should be mentioned that the coatings with AAP-2 exhibited moderate delamination around the scribe (in relation to the others systems; Table 3), but these samples (and the coatings with AAP-1 phosphate; P-AA1) were significantly blistered after their exposition in the salt mist. Additionally, steel corrosion potential values for the extracts of these fillers were lower (–724 mV for AAP-1, –694 mV for AAP-2) in comparison with the reference electrolyte (–653 mV) and other extracts of the nanosized fillers (> –609 mV). The high  $\eta_{TAF}$  values (noted for AAP-2 and AAP-1) were probably the result of a relatively higher P<sub>2</sub>O<sub>5</sub> content and/or water solubility of these phosphates (i.e., a higher anticorrosive components concentration in the AAP-2 and AAP-1 extracts) than the other fillers<sup>12,26</sup>; moreover, the pH value of AAP-2 extract was higher (pH 7.8 due to the higher NH<sub>3</sub> content) in relation to AAP-1 and the rest of the additives (Table 2). A positive influence of basic conditions on anticorrosive features of various phosphates was described in the literature.<sup>7</sup>

**Table 3: Delamination values and blistering degrees of painted steel panels exposed in the salt spray chamber**

Salt spray test duration (h)	P-AA1	P-AA2	P-CAA1	P-CAA2	P-S	P-AAS1	P-AAS2	P-Z
Delamination around the scribe <sup>a</sup> (mm)								
480	5.8 ± 1.6	5.9 ± 1.5	6.2 ± 1.3	4.9 ± 1.4	5.9 ± 2.5	5.7 ± 1.5	4.4 ± 1.2	5.8 ± 1.9
960	9.6 ± 2.2	7.0 ± 2.3	8.5 ± 1.9	6.4 ± 0.8	6.9 ± 1.9	7.3 ± 1.4	6.3 ± 1.0	7.6 ± 2.7
1440	10.5 ± 3	7.6 ± 2.1	11.0 ± 2.3	7.1 ± 1.1	7.9 ± 1.6	7.5 ± 1.3	6.4 ± 1.2	8.4 ± 3.8
Blistering outside the scribe <sup>b</sup>								
480	–	–	–	–	–	–	–	–
960	[2(s2)]	[2(s3)]	[2(s2)]	–	–	–	–	–
1440	[3(s2)]	[2(s3)]	[2(s2)]	–	–	–	–	–

<sup>a</sup>According to EN ISO 4628-8; <sup>b</sup>described as “frequency(size)” of blisters according to EN ISO 4628-2

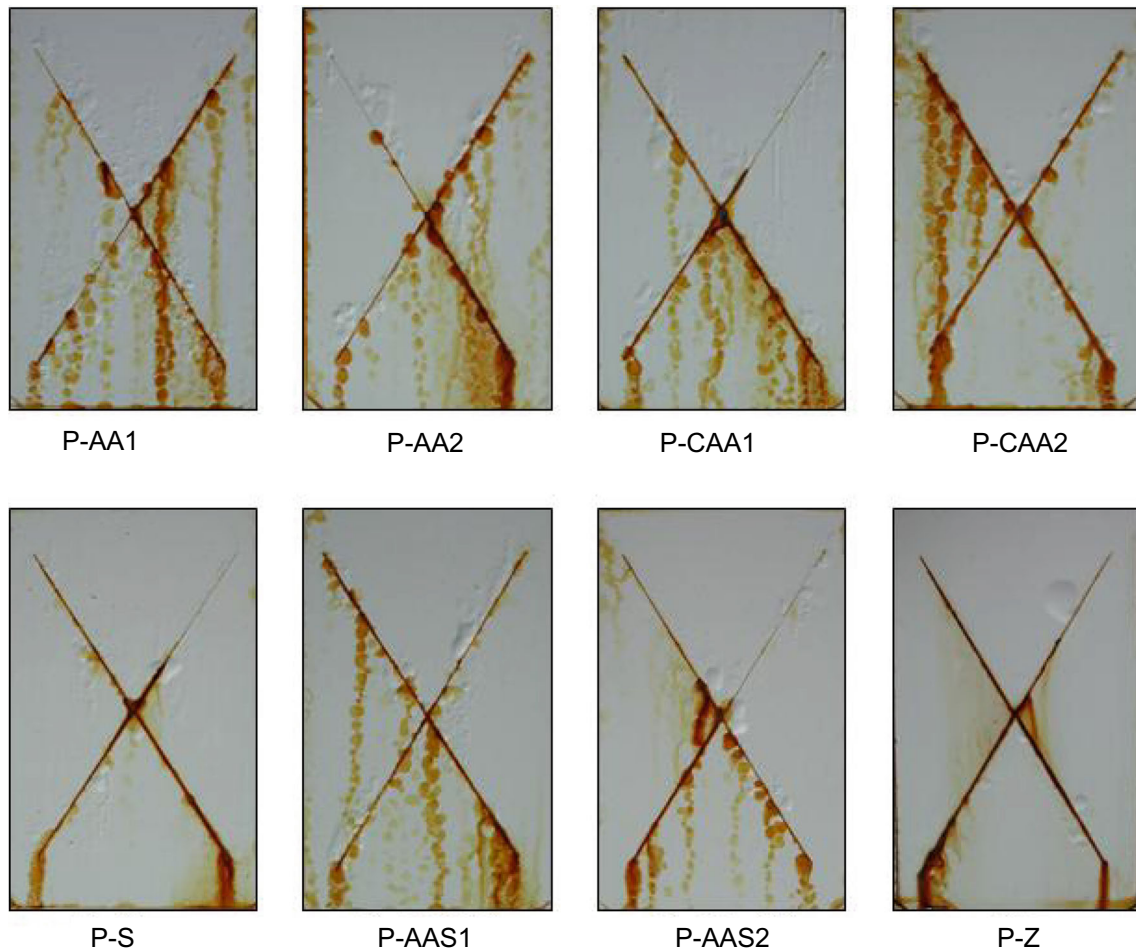


Fig. 9: Macrographs of coated steel samples after exposition for 1440 h in the salt spray chamber

Table 4: Electrochemical noise and Tafel test results for steel immersed in suspensions/extracts of phosphate fillers in 3.5 wt% NaCl aqueous solution

Phosphate acronym	Electrochemical noise test results <sup>a</sup>			Tafel test results <sup>b</sup>		
	Current noise density (nA/cm <sup>2</sup> )	Charge density (mC/cm <sup>2</sup> )	Corrosion inhibition efficiency (%)	Corrosion potential (mV vs. SCE)	Corrosion current density (μA/cm <sup>2</sup> )	Corrosion inhibition efficiency (%)
No phosphate	1595 ± 331	136 ± 24	–	– 653	9.4	–
AAP-1	697 ± 51	56.9 ± 3.2	58	– 724	5.0	47
AAP-2	850 ± 101	71.0 ± 9.2	48	– 694	3.0	68
CAAP-1	190 ± 3	15.5 ± 0.5	89	– 583	5.8	38
CAAP-2	246 ± 19	19.7 ± 2.4	86	– 571	6.1	35
SP	146 ± 39	11.2 ± 3.2	92	– 566	7.4	21
AAP-1 + SP <sup>c</sup>	461 ± 68	36.7 ± 2.7	73	– 609	4.7	50
AAP-2 + SP <sup>c</sup>	389 ± 68	30.6 ± 3.3	78	– 592	6.5	31
ZP	292 ± 62	20.9 ± 5.4	85	– 634	8.5	10

<sup>a</sup>For fillers suspensions; <sup>b</sup>for fillers extracts; <sup>c</sup>mixture of an aluminum ammonium phosphate and strontium phosphate (50/50 m/m)

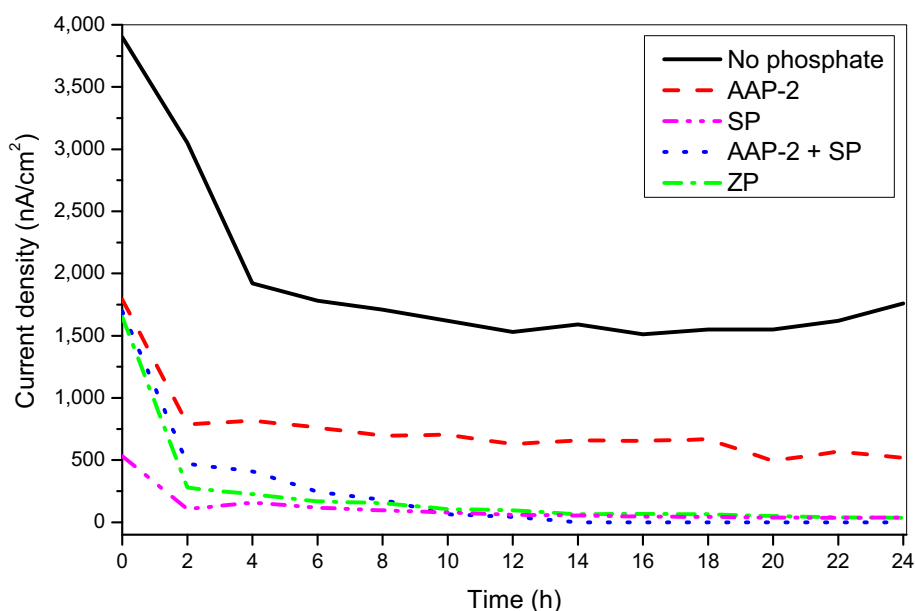


Fig. 10: Variation of current noise density for steel samples immersed in phosphate filler suspensions in 3.5 wt% NaCl aqueous solution

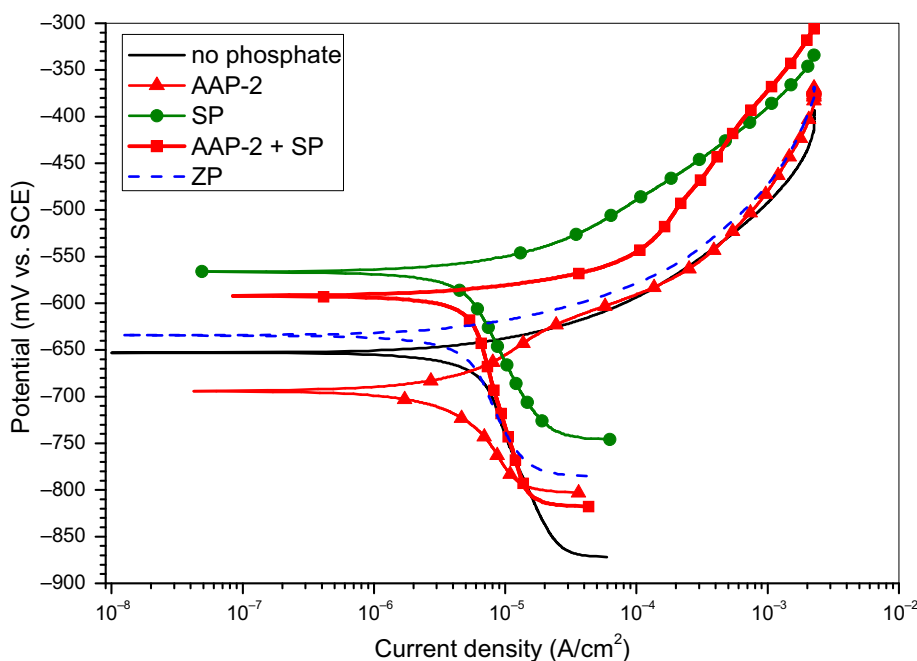


Fig. 11: Potentiodynamic polarization curves for steel immersed in phosphate fillers extracts in 3.5 wt% NaCl aqueous solution

Water solubility of the phosphates was not a crucial parameter in the case of electrochemical noise experiments. Important anticorrosive components in electrolytes were continuously supplemented during the tests from dispersed phosphate particles; as can be seen, the highest  $\eta_{EN}$  values were recorded for the fillers exhibiting moderate or relatively low water solubility (i.e., SP, CAAP-1, CAAP-2, ZP; Table 4).

XRD analysis of steel corrosion products (formed during the EN tests) revealed the sole presence of crystalline lepidocrocite ( $\gamma$ -FeOOH) (diffraction graphs not presented). It should be noted that the highest amounts of rust deposits were observed for the steel substrates tested in AAP-1 and AAP-2 suspensions (exemplary macrographs are collected in Fig. 12), i.e., in the electrolytes exhibiting the lowest  $\eta_{EN}$

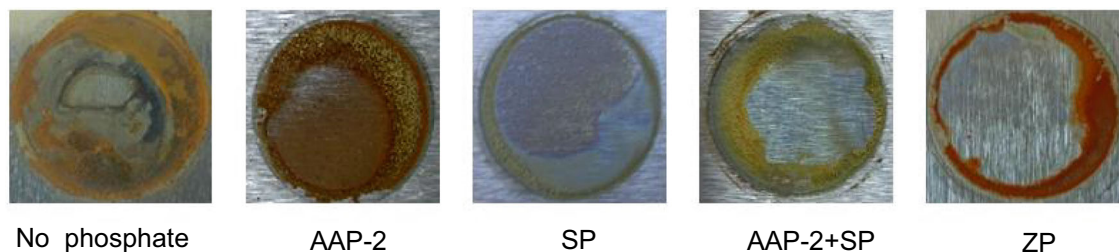


Fig. 12: Macrographs of steel panels after electrochemical noise experiments

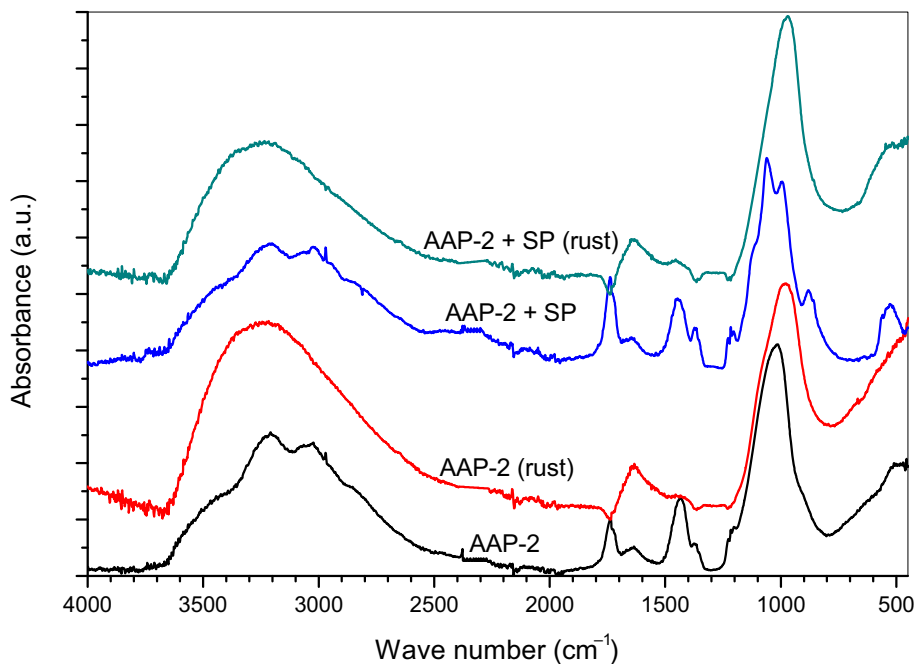


Fig. 13: FTIR spectra for the phosphate fillers (AAP-2 and AAP-2 + SP) as well as corrosion products of steel immersed in the filler suspensions in 3.5 wt% aqueous solution (the sediments collected after electrochemical noise tests)

(Table 4). On the other hand, FTIR analysis showed that the corrosion products (exemplary spectra are presented in Fig. 13) contained lepidocrocite (bands at  $493\text{--}547\text{ cm}^{-1}$ ),<sup>2</sup>  $\text{PO}_4^{3-}$  ( $493\text{--}547$  and  $964\text{--}992\text{ cm}^{-1}$ ),<sup>27,28</sup> goethite ( $\alpha\text{-FeOOH}$ ,  $964\text{--}992\text{ cm}^{-1}$ ),<sup>2</sup>  $\text{P}=\text{O}$ <sup>29</sup> or  $\text{CO}_3^{2-}$  ( $1427\text{--}1460\text{ cm}^{-1}$ ),<sup>2,27,30</sup>  $\text{H}_2\text{O}$  ( $1634\text{--}1648$  and  $3249\text{--}3300\text{ cm}^{-1}$ ),<sup>2,28,29</sup> or hydroxyl functional compounds ( $3249\text{--}3300\text{ cm}^{-1}$ ).<sup>2,29</sup> The mentioned carbonates were probably created from  $\text{CO}_2$  dissolved in the phosphate suspensions (the electrolytes were air-saturated during the EN experiments). Nevertheless, described bands were also observed on FTIR spectra of the powdered phosphate fillers (Fig. 13); thus, the corrosion products might contain the fillers particles as well. In the case of deposits generated in the suspensions of ammonium-modified phosphate fillers, i.e., AAP, CAAP, AAP/SP, an extra (small and wide) peak at  $1243\text{--}1366\text{ cm}^{-1}$  was recorded. Perhaps that band represents  $\text{NH}_4^+$  cations.<sup>27</sup> The most intensive peaks representing  $\text{CO}_3^{2-}$

and  $\text{NH}_4^+$  were noted for the sediments created on the steel tested in the AAP-2/SP mixture suspension. The polyurethane paint filled with that mixture exhibited the best anticorrosive features after the salt spray test. Arguably, migration of  $\text{NH}_4^+$  to the substrate (coated with P-AAS2 and exposed in the salt spray chamber) resulted in an increment of a local pH value and inhibition of steel corrosion.<sup>31</sup>

## Conclusions

Anticorrosive 2 K solventborne polyurethane paints containing novel nanosized aluminum ammonium phosphates (AAP) or calcium aluminum ammonium phosphates (CAAP) were prepared and tested. For comparison, coating systems based on a nanosized strontium phosphate (SP), mixtures of AAP and SP (AAP/SP), and a micro-sized zinc phosphate (ZP) were investigated. Taking into consideration test results of

the liquid compositions and coatings (with PVC/CPVC = 0.55) cured on a steel substrate, the following conclusions can be drawn:

- The paints with the ammonium-modified phosphates exhibited similar (CAAP, AAP/SP) or slightly higher viscosity (AAP) than the composition based on ZP. The lowest viscosity was noted for the paint filled with SP.
- Cured coatings with the nanofillers (mainly AAP-type) reached markedly higher gloss and adhesion as well as slightly higher hardness in relation to the system filled with ZP.
- The primer-less coatings containing AAP/SP, SP or a selected CAAP filler exhibited reduced delamination around the scribe (6.4–7.9 mm after 1440 h in a salt spray chamber) in relation to the coatings with ZP (8.4 mm); the best protective features were registered for the AAP/SP-filled sample.
- EIS test results revealed markedly higher barrier properties of cured coatings based on a selected AAP filler in comparison with the samples with the other phosphates. These features were affected by phosphate particles size, their water solubility and volumetric content in a coating.
- The highest steel corrosion inhibition efficiency values were registered for aqueous extracts of the AAP fillers and a selected AAP/SP mixture (results for potentiodynamic polarization tests) and for aqueous suspensions of SP and the CAAP-type phosphates (electrochemical noise experiments). The results of the electrochemical measurements did not correlate with the salt spray chamber test outcomes; however, these experiments confirmed a better barrier/anticorrosive efficiency of the nano-sized zinc-free phosphate (and related coatings) in comparison with the system based on the micro-sized zinc phosphate.

**Acknowledgments** Work financed by the National Centre for Research and Development (NCBiR, Poland) under the “Tango” Project (TANGO1/266477/NCBR/2015; 2015-2018). Some of the results were presented at “Antykorozja” scientific conference (29-31.03.2017, Ustroń-Jaszowiec, Poland).

**Open Access** This article is distributed under the terms of the Creative Commons Attribution 4.0 International License (<http://creativecommons.org/licenses/by/4.0/>), which permits unrestricted use, distribution, and reproduction in any medium, provided you give appropriate credit to the original author(s) and the source, provide a link to the Creative Commons license, and indicate if changes were made.

## References

1. Alibakhshi, E, Ghasemi, E, Mahdavian, M, “Corrosion Inhibition by Lithium Zinc Phosphate Pigment.” *Corr. Sci.*, **77** 222–229 (2013)
2. Alibakhshi, E, Ghasemi, E, Mahdavian, M, “Sodium Zinc Phosphate as a Corrosion Inhibitive Pigment.” *Prog. Org. Coat.*, **77** 1155–1162 (2014)
3. Abd El-Ghaffar, M, Youssef, E, Ahmed, N, “High Performance Anticorrosive Paint Formulations Based on Phosphate Pigments.” *Pig. Res. Technol.*, **33** 226–237 (2004)
4. Roselli, S, Romagnoli, R, Deyá, C, “The Anti-Corrosion Performance of Water-Borne Paints in Long Term Tests.” *Prog. Org. Coat.*, **109** 172–178 (2017)
5. Heydarpour, M, Zarrabi, A, Attar, M, Ramezanzadeh, B, “Studying the Corrosion Protection Properties of an Epoxy Coating Containing Different Mixtures of Strontium Aluminum Polyphosphate (SAPP) and Zinc Aluminum Phosphate (ZPA) Pigments.” *Prog. Org. Coat.*, **77** 160–167 (2014)
6. Naderi, R, Arman, S, Fouladvand, S, “Investigation on the Inhibition Synergism of New Generations of Phosphate-Based Anticorrosion Pigments.” *Dyes Pigm.*, **105** 23–33 (2014)
7. Kowalczyk, K, Łuczka, K, Grzmil, B, “Preparation and Characterization of Anticorrosion Polyurethane Paints and Coats Based on Novel Zn-Free Phosphates.” *J. Coat. Technol. Res.*, **12** 153–165 (2015)
8. Kowalczyk, K, Łuczka, K, Grzmil, B, Spychaj, T, “Anticorrosive 2 K Polyurethane Paints Based on Nano- and Microphosphates with High Dispersing Additive Content.” *Prog. Org. Coat.*, **76** 1088–1094 (2013)
9. Kowalczyk, K, Łuczka, K, Grzmil, B, Spychaj, T, “Anticorrosive Polyurethane Paints with Nano- and Microsized Phosphates.” *Prog. Org. Coat.*, **74** 151–157 (2012)
10. Kalenda, P, Kalendová, A, Veselý, D, “Properties of Anticorrosion Pigments Depending on Their Chemical Composition and PVC Value.” *Pig. Res. Technol.*, **35** (4) 188–199 (2006)
11. Hernández, M, Genescá, J, Uruchurtu, J, Galliano, F, Landolt, D, “Effect of an Inhibitor Pigment Zinc-Aluminum-Phosphate (ZAP) on the Corrosion Mechanisms of Steel in Waterborne Coatings.” *Prog. Org. Coat.*, **56** 199–206 (2006)
12. Bethencourt, M, Botana, F, Marcos, M, Osuna, R, Sánchez-Amaya, J, “Inhibitor Properties of “Green” Pigments for Paints.” *Prog. Org. Coat.*, **46** 280–287 (2003)
13. Kalendová, A, “Comparison of the Anticorrosion Efficiencies of Pigments Based on Condensed Phosphates and Polyphosphosilicates.” *Anti-corr. Meth. Mater.*, **50** 82–90 (2003)
14. del Amo, B, Romagnoli, R, Deyá, C, González, J, “High Performance Water-Based Paints with Non-Toxic Anticorrosive Pigments.” *Prog. Org. Coat.*, **45** 389–397 (2002)
15. Kalendová, A, Veselý, D, Brodinová, J, “Anticorrosive Spinel-Type Pigments of the Mixed Metal Oxides Compared to Metal Polyphosphates.” *Anti-Corr. Meth. Mater.*, **51** 6–17 (2004)
16. Jašková, V, Kalendová, A, “Anticorrosive Coatings Containing Modified Phosphates.” *Prog. Org. Coat.*, **75** 328–334 (2012)

17. Kalendová, A, “Comparison of the Efficiencies of Anticorrosive Pigments Based on Chemically Modified Phosphates.” *Anti-Corr. Meth. Mater.*, **49** 364–372 (2002)
18. Gorodylová, N, Dohnalová, Ž, Šulcová, P, Bělina, P, Vlček, M, “Influence of Synthesis Conditions on Physicochemical Parameters and Corrosion Inhibiting Activity of Strontium Pyrophosphates  $\text{SrM}^{\text{II}}\text{P}_2\text{O}_7$  ( $\text{M}^{\text{II}} = \text{Mg}$  and  $\text{Zn}$ ).” *Prog. Org. Coat.*, **93** 77–86 (2016)
19. Ahmed, N, Mohamed, M, Mabrouk, M, ElShami, A, “Novel Anticorrosive Pigments Based on Waste Material for Corrosion Protection of Reinforced Concrete Steel.” *Constr. Build. Mater.*, **98** 388–396 (2015)
20. Zin, I, Lyon, S, Pokhmurskii, V, “Corrosion Control of Galvanized Steel Using a Phosphate/Calcium Ion Inhibitor Mixture.” *Corr. Sci.*, **45** 777–788 (2003)
21. Naderi, R, Mahdavian, M, Darvish, A, “Electrochemical Examining Behavior of Epoxy Coating Incorporating Zinc-Free Phosphate-Based Anticorrosion Pigment.” *Prog. Org. Coat.*, **76** 302–306 (2013)
22. Spychaj, T, Spychaj, S, *Water-Thinnable Paints and Adhesives*. WNT, Warsaw, 1996
23. Gawri, S, Balakrishnan, K, “The Effect of the PVC/CPVC Ratio on the Corrosion Resistance Properties of Organic Coatings.” *Prog. Org. Coat.*, **23** 363–377 (1994)
24. Murray, J, “Electrochemical Test Methods for Evaluating Organic Coatings on Metals: an Update. Part III: Multiple Test Parameter Measurements.” *Prog. Org. Coat.*, **31** 375–391 (1997)
25. <http://www.phys.uri.edu/gerhard/PHY204/tsl106.pdf> (26.11.2017)
26. Hernández, M, Galliano, F, Landolt, D, *Corros. Sci.*, **46** 2280–2300 (2004)
27. Stuart, B, *Infrared Spectroscopy: Fundamentals and Applications*. Wiley, Chichester, 2004
28. Fernandes, K, Alvarenga, E, Brandão, P, Lins, V, “Infrared-Spectroscopy Analysis of Zinc Phosphate and Nickel and Manganese Modified Zinc Phosphate Coatings on Electro-galvanized Steel.” *R. Esc. Minas*, **64** 45–49 (2011)
29. Alibakhshi, E, Ghasemi, E, Mahdavian, M, “A Comparison Study on Corrosion Behavior of Zinc Phosphate and Potassium Zinc Phosphate Anticorrosive Pigments.” *Prog. Color Colorants Coat.*, **5** 91–99 (2012)
30. Daik, R, Lajnef, M, Amor, S, Elgharbi, S, Meddeb, H, Abdessalem, K, Férid, M, Ezzaouia, H, “Application of Gettering Process on the Improvement of the Structural and Mineralogical Properties of Tunisian Phosphate Rock.” *J. Mater. Sci. Eng.*, **5** 222–227 (2015)
31. Uhlig, H, *Corrosion and Corrosion Control*. WNT, Warsaw, 1976